Atmospheric Effects on Fate of Aerially Applied Agricultural Sprays

[1]B. K. Fritz, [1]W. C. Hoffmann
[1]USDA-ARS, College Station, TX 77845
(Corresponding author: Address: 2771 F&B Road, College Station, TX 77845. E-mail: brad.fritz@ars.usda.gov)

ABSTRACT

The deposition and drift of aerially applied crop protection materials is influenced by a number of factors including equipment setup and operational parameters, spray material, and meteorological conditions. This work focuses on evaluating the meteorological influences on the transport and ultimate fate of aerially applied sprays. There was no single meteorological factor that dominated the downwind transport of the spray treatments replicated in this study. Generally, lower relative humidity decreased downwind deposition and the amount of spray unaccounted for due to evaporative effects. Increasing wind speeds decreased both in-swath deposition and downwind deposition, and increased the amount of mass unaccounted for. Increases in stability were only moderately correlated to downwind deposition and to flux measurements past 40 m. Though this data set covers a limited range of meteorological conditions, the trends hold from the standpoint of the system physics, and provide applicators with a further understanding of the relationships between spray transport and deposition and local meteorology.

Keywords. Aerial application, aerial spraying, spray deposition, mass balance, US.

1. INTRODUCTION

The Environmental Protection Agency (EPA) defines spray drift as the physical movement of applied spray materials through the air to any off-target site. Airborne spray leaving the targeted area reduces the applied dosage, and has the potential to create crop damage, human hazards or other detrimental environmental impacts. The deposition and drift of aerially applied crop protection materials is influenced by a number of factors including equipment setup and operational parameters, spray material characteristics, and meteorological conditions. This work focused on evaluating the meteorological influences on the transport and ultimate fate of applied materials.

Bird (1995) compiled and examined a number of aerial application field tests that were available in the literature and extrapolated the reported data to reflect a 20 swath application with deposition downwind expressed as a percent of the total applied. She noted that wind speed, application height, and drop size were the dominant factors influencing off-target drift. Bird et al. (1996) further observed that given similar stability conditions, downwind deposition increased with increasing wind speeds, but that higher wind speeds tended to reduce stability and, therefore, the effect of stability on drift.

Karsky and Thomasson (1989) observed little correlation of drift measured on vertical cylindrical spot collectors to stability or wind speeds, but they observed a high positive correlation of airborne drift to relative humidity. Even with the weak correlation, Karsky and Thomasson (1989) noted that the downwind drift increased with increasing wind speed. Payne and Thompson (1992) showed that for downwind distances less than 50 m, ground deposits were lesser under low wind speeds (0.5 to 2 m/s at 2 m height) and slightly stable conditions (Richardson number, Ri = 0.01 to 0.2) as compared to intermediate wind speeds (approx. 3-4 m/s at 2 m height) and unstable conditions (Ri < 0.0). They further observed that beyond 100 m ground deposition was either reduced, or unaffected by increases in wind speed or decreases in stability, with the lowest observed deposition amounts occurring under higher wind speeds coupled with an unstable boundary layer. This was also observed in modeling results by Craig et al. (1998).

Researchers have reported that on-target deposition may be less than 50% of that applied (Ware et al., 1970 and Willis and McDowell, 1987) and that 15-50% of the applied material may remain suspended and transported off the site of application (Frost, 1973 and Van den Berg et al., 1999). Bird (1995) observed that at approximately 30 m downwind the deposition ranged from 1 to 10% of the total applied and at approximately 400 m downwind deposition ranged from 0.02 to 1% of the total applied. Salyani et al (2007) in a mass balance of ground sprays in a citrus orchard were able to account for up to 80% of total applied material. Part of the material unaccounted for in these studies was likely due to methodological problems and collection efficiency issues.

The objective of this study was to contribute to the available literature additional understanding of the influences of meteorological conditions on the deposition, transport, and mass accountability of aerially applied sprays.

2. MATERIALS AND METHODS

Twelve aerial application trials were conducted. Details of the application equipment setup, meteorological monitoring, study layout, spray accountability, sample collection and processing and statistical analysis are discussed in the following sections.

2.1 Application Equipment Setup

An AirTractor AT-402B was used for all applications and was operated at 209 km/h with an aircraft spray boom height of 2.4 m, a swath width of 20 m, and a spray rate of 28 L/ha. The spray solution consisted of water, Trition X-100 surfactant at 0.1% v/v, and Caracid Brilliant Flavine FFN fluorescent dye at 15 g/ha. Boom setup was configured to produce a FINE droplet spectrum based on ASAE Standard S572 (ASAE, 2000). Application parameters and nozzle setups were selected to generate desired droplet spectrums using USDA-ARS Aerial Spray Nozzle Models (http://apmru.usda.gov/downloads/downloads.htm). Twenty-five CP-03 nozzles (CP Products, Inc., Mesa, AZ) were configured with the 3.175 mm orifice and a 90° deflection angle, and were operated at 207 kPa. Based on the USDA-ARS aerial spray models, this

configuration results in a VMD (volume median diameter, DV0.5, the diameter of droplet such that 50% of the total volume of droplets is in droplets of smaller diameter) of 236 μm; a V<200μm (Percent of spray volume contained in droplets less than 200 μm in diameter) of 34%; and a V<100μm (Percent of spray volume contained in droplets less than 100 μm in diameter) of 14%.

2.2 Meteorological Monitoring

Meteorological data were monitored throughout the tests using a meteorological tower. The tower was located approximately 100 meters downwind of the flight line directly alongside the sampling line. The monitoring tower was oriented such a north reading on the wind direction sensors corresponded to a direction perpendicular to the flight line. The meteorological tower measured one-minute averages of wind speed and direction (RM Young model 05701 Wind Monitor-RE), and temperature (RM Young model 43347VC Temperature Probes in a model 43408 aspirated radiation shield match calibrated with relative difference accuracy of 0.1 °C) at 2.5, 5, and 10 meters. Relative humidity was measured with an RM Young model 71372 temperature/relative humidity sensor. The measured data was used to calculate the gradient Richardson number between 2.5 and 10 m for each replication (Eq. 1).

$$Ri = \frac{g\left(dT/dz\right)}{T\left(du/dz\right)^2} \qquad \text{(Bache and Johnstone, 1992)} \quad (1)$$

Where:

	Ri	=	gradient Richardson number
	g	=	acceleration due to gravity, 9.1 m/s2
	dT/dz	=	temperature gradient between 9.1 and 1.8 m, K/m
	du/dz	=	wind speed gradient between 9.1 and 1.8 m, 1/s
	T	=	air temperature, K

2.3 Study Layout

The flight line and downwind sampling locations were located in the center of a large, (approx. 70 ha square) flat, field of wheat stubble (10 to 20 cm tall). Three sub-samples of mylar collectors (A, B, and C) at multiple downwind distances were used to capture ground deposition of spray (Figure 1). The mylar cards (10x10 cm) were placed on square metal plates positioned flat on the ground. Monofilament nylon screen cylinders (20x20 cm squares rolled into cylinders with a frontal area of 131 cm^2 – 20.3 cm tall by 6.5 cm wide) positioned at multiple heights (0.3, 3, and 6 m) and downwind distances on sampling towers collected the airborne portion of the spray (Figure 1). The screens had 16 fibers/cm and a porosity of 56% (Filter Fabrics Inc, Goshen, Ind. Part number 1420). Additionally, water sensitive papers (WSP) were placed flat on the ground at downwind distances of 10, 20, 30, 40, 50, 75, 100, 150, and 200m, as well as at 0.3 and 6 m height on the sampling towers and oriented vertically facing into the wind (frontal area of 19.4 cm^2 – 7.6 cm tall by 2.5 cm wide) (Figure 1).

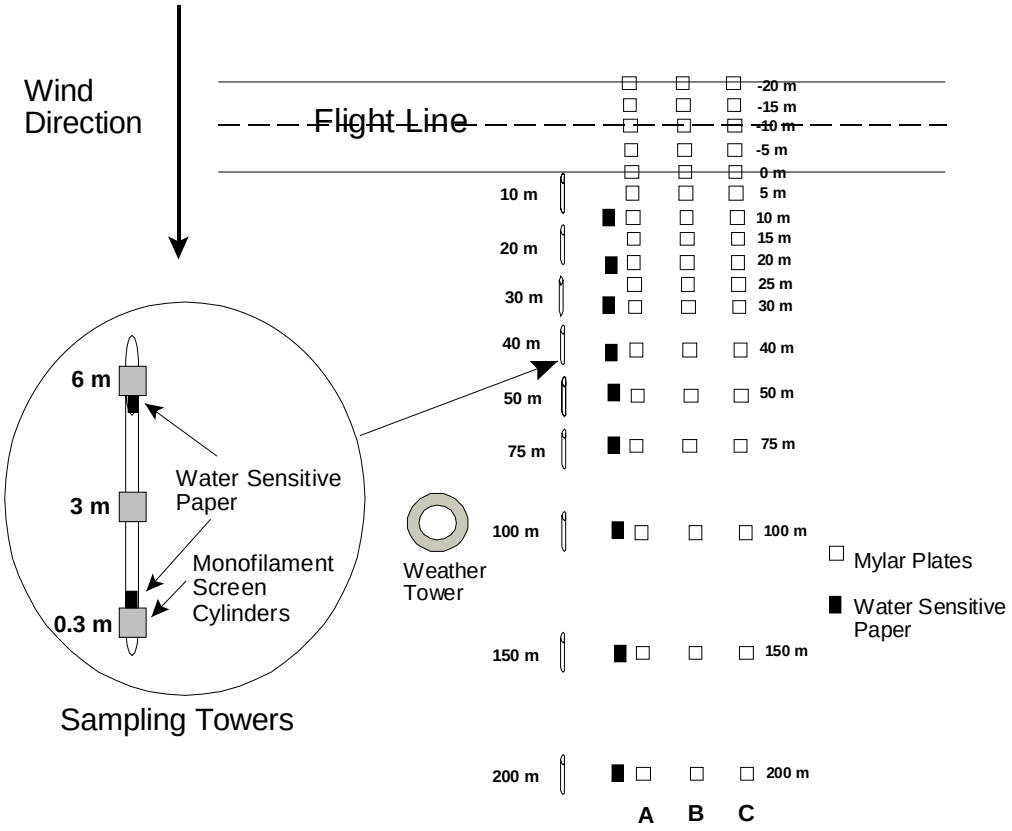

Figure 1. Test layout for field studies.

Replications 1 through 6 were completed in the morning as soon as the pilot judged it safe to fly and replications 7 through 12 were completed in the evening prior to darkness. The aircraft made two passes, one with the left wing on the downwind side and another with the right wing on the downwind side over the same spray line. Spray was initiated 300 m before the sampling line and stopped 300 m after the sampling line.

2.4 Sample Collection and Processing

Following each replication, ten minutes were allowed for spray material to travel downwind prior to collection of all sampling media. Mylar cards and nylon screen cylinders were collected and immediately placed in labeled plastic bags, which were then placed and sealed in an ice chest for transport to the laboratory. WSPs were collected, allowed to dry (if needed) and placed in plastic film negative sleeves for protection and transport. Analysis consisted of pipetting 20 or 40 ml of an 100% ethanol wash into each bag, agitating the sample bag (approx. 20 sec for mylar and 45 sec for screen), and decanting 6 ml into a cuvette. The dye concentration (µg/ml) of samples and tank mixture were measured using a spectrofluorometer (Shimadzu, Model RF5000U, Kyoto, Japan) and reference standards. The sample concentration was multiplied by the wash volume and divided by the effective sample area to get µg of dye/cm^2. Tracer recovery

losses on the mylar and screen samples were determined using 20 clean samples of both mylar and nylon screen cylinders that were spiked with a known quantity of tank mix material. Samples were then washed and analyzed following the same protocol as discussed above. Mylar samplers showed average recovery losses of 5% ($\sigma^2 = 4.9$) and nylon screen cylinders showed average recovery losses of 15% ($\sigma^2 = 5.1$).

WSP samples were processed with computerized image analysis developed in house using IMAQ Vision Builder v5 (National Instruments, Austin, Texas) to determine droplet stain size. Stain size, stain diameter, and minimum stain dimension were determined in two 0.75 cm^2 sample areas on each card. Each stain in the sample area was converted to droplet diameter using our experimentally determined spread factor (0.54*stain diameter – $8.5x10^{-5}$*stain $diameter^2$, unpublished data).

2.5 Spray Accountability

Spray accountability, or mass balance, provides applicators and researchers with a way of determining how much of the spray released from a sprayer reaches the intended target. By comparing the total amount of spray (i.e. dye) measured in-swath, downwind, and in the airborne component of the spray with the total amount of spray applied, spray accountability was calculated for these studies. Prior to the mass balance analysis, spray deposition and flux data had to be corrected based on the difference between the wind direction and the downwind sampling line. For replications where the wind direction is not parallel to the downwind sampling line, not only the distance from the release point of the spray to the sampling locations changes, but the source strength changes as the plume becomes narrower (Thistle et al, 2005). Therefore, the mylar and nylon screen deposition data were corrected for wind direction by adjusting the source strength using a line source projection as describe by Thistle et al. (2005).

2.5.1 Total Applied

Calculation of the actual total mass of dye applied required accounting for variation in spray rates due to actual groundspeed and measured dye concentrations in the spray material. Actual groundspeed was determined from GPS data recorded with the Del Norte Flying Flagman (Hemisphere GPS, Euless, Texas) while the spray material dye concentration was determined from analysis of sampled tank mix material. The actual dye application rate (μg/s) was determined using the spray liquid flowrate (determined based on 25 CP-03 nozzles set to the 3.2 mm orifice operating at 207 kPa for a total flowrate of 3.24 L/s) and the actual dye concentration in the spray material. To perform the mass balance, the actual mass of dye applied, with respect to a length scale corresponding to the mylar sampler length (10 cm), was calculated by multiplying the dye application rate (μg/s) by the time required (seconds) for the aircraft to cover 10 cm. The resulting value (μg of dye) corresponds to the mass of dye applied over a 10 cm length in one pass. Analysis of tank mix samples used in replications one through six showed a dye concentration of 1114 μg/mL, and a dye concentration of 1222 μg/mL for the tank mix used in replications seven through twelve. GPS recorded groundspeeds varied between 60 and 64 m/s.

2.5.2 In-Swath Portion

Based on the total amount of dye applied, $M_{applied}$ as pictured in Figure 2, the in-swath and total downwind deposition and the downwind flux measurements were expressed as a percentage of the total applied dye. The total deposition in-swath was calculated based on the mylar measured deposition values ($\mu g/cm^2$) from -20 to 0 m. The sub-samples (A, B, and C) at each distance were averaged and integrated over a total swath area corresponding to the width of the mylar sampler (total swath area defined as the mylar length, 10 cm, multiplied by the swath width, 20 m) to return a total mass of dye, $D_{In\text{-}swath}$ in Figure 2, deposited in-swath. This was then corrected for degradation (10%) (Hoffmann et al., 2007) and recovery losses (5%) by dividing by 0.85. The same degradation value was used for all samples as all samples were collected using multiple field crews within a five minute period and thus had similar exposure times. The in-swath deposition in terms of fraction of applied is calculated as the total mass deposited in-swath, $D_{In\text{-}swath}$, over the total mass applied, $M_{applied}$.

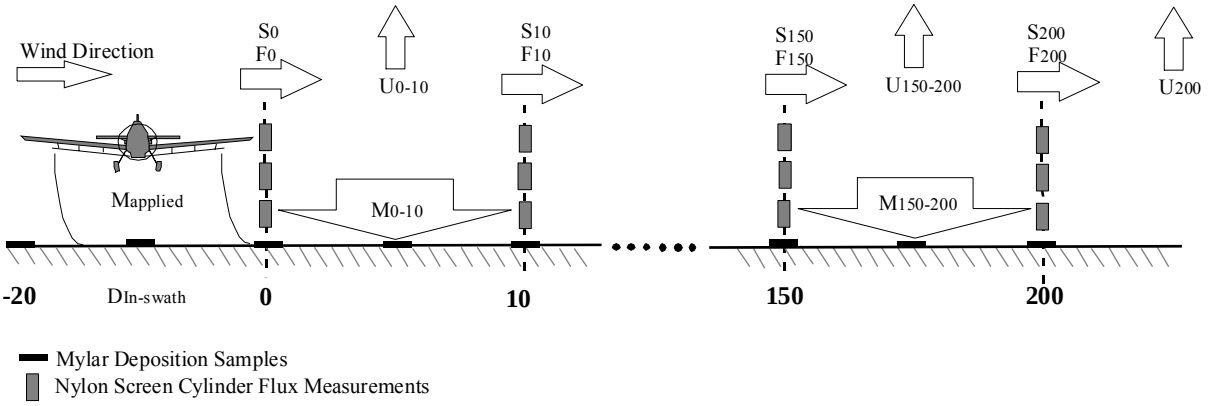

Figure 2. Spray accountability calculation flowchart. Note: Figure is not to scale. Where M_i = mass of dye deposited at i location; S_i = mass flux based on screen measured data at distance i; F_i = calculated dye flux ($\mu g/cm^2$) based on mylar deposition data past distance i; U_i = dye unaccounted for past distance i.

2.5.3 Downwind Portion

Downwind deposition results were also expressed in terms of fraction of total applied dye. Similar to the in-swath deposition, the mylar deposition sub-samples (A, B, and C) were averaged at each distance and integrated over a total distance of interest. For example, deposition from 0 to 10 m downwind was calculated based on the mylar measured deposition values at 0, 5, and 10 m distances. The deposition values were expressed in terms of fraction of applied by dividing the mass deposited over a given interval (i.e. $M_{0\text{-}10}$ is the mass deposited from 0 to 10 m) over the total mass applied, $M_{applied}$. These calculations were performed from 0 – 10 , 10 – 20, 20 – 30, 30 – 40, 40 – 50, 50 – 75, 75 – 100, 100 – 150, and 150 – 200 m to return

the incremental depositions, and over the total sampling line, 0 – 200 m, to return the total integrated downwind deposition.

2.5.4 Airborne Portion

The screen collected data (μg dye/cm^2) were integrated over a total vertical flux area corresponding to the sampling height (6.1 m) by the mylar width (10 cm) to return a measure, F_i, of the total suspended dye mass that moved past a given distance as a result of the spray pass made each replication. While flux is normally expressed as a mass per area per time, here time is implicit of the total time required for the finite amount spray material applied to move from the application swath past the downwind locations. Therefore, the screen measured mass per area is a total flux for each replication. The mylar width was used, instead of the screen sampler width, to reflect a mass flux over the same application length for the mass balance calculations. The calculated airborne dye mass values were adjusted for degradation and recovery rates and screen collection efficiency. The screen cylinders have a spray collection efficiency varying from 9% and 40% for a spray with a $D_{V0.5}$ of 20 μm in air velocities of 0.3 and 1.0 m/s, respectively (Fritz and Hoffmann, 2008). Droplets measured on the WSP in these studies indicated suspended droplet sizes ranging from near 200 μm to less than 10 μm, with the droplet $D_{V0.5}$ decreasing with downwind distance. Based on work by May and Clifford (1967), collection efficiency increases with increasing droplet size. To account for this, the screen collection efficiencies varied linearly from 11% at 10 m to 6% at 200m for replications 1-6 and from 50% at 10 m to 30% at 200m for replications 7-12. These efficiencies were determined based on the WSP measured droplet spectrum and measured collection efficiencies as reported by Fritz and Hoffmann (2008).

The airborne dye mass values were further adjusted by a factor of 0.75 reflecting the dye degradation (10%) (Hoffmann et al., 2007) and recovery losses (15%) for the screen samples. The resulting airborne dye mass data was divided by the total dye applied to express the results as a fraction of applied. For example, the integrated flux (μg dye/cm^2), from 0 to 6.1 m height, past the 10 m location was multiplied by the total vertical flux area (0.61 m^2) resulting in total measured mass of airborne dye transported past the 10 m sampling location, F_{10} in Figure 2. Dividing F_{10} by $M_{applied}$ expresses the data as a fraction of total applied dye.

2.5.5 Unaccounted Portion

The mass accounting examined the ground deposition versus the total mass of dye applied to determine the mass of dye remaining airborne. For example, S_{10} in Figure 2 represents the mass of dye remaining airborne and was calculated as the total mass applied minus the mass deposited in-swath and the mass deposited from 0 to 10 m ($S_{10} = M_{applied} - D_{In\text{-}swath} - M_{0\text{-}10}$). This values differs from F_{10}, in that it is the calculated mass remaining suspended and not the measured mass suspended. The mass of dye unaccounted for is the difference between the two. For example, The unaccounted for mass fraction from 0 to 10 m, $U_{0\text{-}10}$ in Figure 2, is calculated as the difference between S_{10} and F_{10} and is converted to a fraction of applied by dividing by $M_{applied.}$ The overall mass unaccounted for is this difference at the final sampling location (200m). This unaccounted for mass was also expressed as percent of total applied by dividing by the total mass

applied ($[S_{200}-F_{200}]/M_{applied}$). Note S_0 represented the amount of suspended material that did not deposit in-swath and is calculated as the total mass applied, $M_{applied}$, minus that deposition in-swath, $D_{In\text{-}swath}$.

2.6 Statistical Analyses

All correlation analyses were performed using the PROC CORR procedures in SAS (SAS Inc., Cary, NC). This procedure computed the Pearson's Correlation Coefficient between variables of interest. The PROC REG procedure was used to find the best fit models.

3. RESULTS

3.1 Meteorological Data

Data recorded for each test are presented in Table 1. Note that the large values for Ri were due to the small difference in wind speeds at the two measurements heights.

Table 1. Meteorological data measured and calculated for each test replication.

Rep	Time of Acquisition	Temp. at 10 m (°C)	Temp. at 2.5 m (°C)	Relative Humidity (%)	Wind Speed at 10 m (m/s)	Wind Speed at 2.5 m (m/s)	Ri[1]	Wind Direction at 5 m	Theta[2]
1	7:16 am	22.0	21.5	95.7	0.6	0.2	0.82	207.5	-27.5
2	7:43 am	22.8	23.0	92.1	0.7	0.4	-0.77	112.8	67.2
3	8:02 am	23.9	24.2	88.7	1.0	0.9	-3.4	125.3	54.7
4	8:18 am	24.6	24.8	86.2	0.8	0.8	-717	134.5	45.5
5	8:35 am	25.5	25.8	82.7	1.1	0.9	-1.8	156.6	23.4
6	8:50 am	26.2	26.6	79.0	0.9	0.9	-22	162.5	17.5
7	7:04 pm	34.3	34.5	37.8	3.1	2.3	-0.030	126.1	53.9
8	7:20 pm	34.2	34.1	38.7	3.0	2.2	0.048	124.9	55.1
9	7:36 pm	33.8	33.5	42.1	2.9	1.9	0.081	138.6	41.4
10	7:52 pm	33.7	33.3	42.2	3.3	2.1	0.086	178.2	1.8
11	8:08 pm	33.1	32.6	44.5	3.3	2.1	0.11	171.5	8.5
12	8:24 pm	32.4	31.4	48.3	2.4	1.4	0.22	172.7	7.3

[1] Richardson's number as calculated using Equation 1.
[2] Theta equals 180 minus the wind direction at 5 m and indicates the angle between the downwind sampling line and the wind direction.

3.2 Deposition

The integrated in-swath deposition expressed as mass and fraction of applied, and the integrated downwind deposition from 0 to 200 m expressed as total mass and fraction of applied, are shown in Table 2.

Table 2. Measured dye deposition in-swath and downwind of application.

Rep	Total Dye Applied (mg)	Integrated Deposition In-swath (mg)	Integrated Deposition In-swath (% of Applied)	Integrated Downwind Deposition, 0-200 m (mg)	Integrated Downwind Deposition, 0-200 m (% of Applied)	% of Spray not Measured by Ground Deposits	Total Accountancy (% of Applied)
1	11.6	8.4	73	2.9	25	2	98
2	11.2	8.8	78	1.9	17	5	95
3	11.6	6.5	56	3.8	33	11	89
4	11.3	7.4	66	2.5	22	12	88
5	11.8	7.1	60	2.0	17	23	77
6	11.1	5.6	51	2.2	20	29	71
7	13.2	5.1	38	2.9	22	40	60
8	12.7	7.7	60	1.7	13	27	78
9	12.3	4.2	34	2.0	15	51	49
10	12.3	4.9	40	1.3	10	50	50
11	12.5	4.2	33	1.6	12	55	45
12	12.7	5.7	45	1.3	15	40	60

The downwind deposition, as measured by the horizontal mylar cards, was also expressed incrementally with respect to distance in terms of percent of the total applied (Table 3). The total deposition downwind from 0 to 200 m, in terms of mass and a percent of applied, the percent of material not measured by the ground deposits (in-swath and downwind), and the total accountancy were also calculated (Table 3).

Table 3. Incremental deposition by distance and replication expressed as percentage of applied.

		Downwind Distance (m)									
	Rep	0-10	10-20	20-30	30-40	40-50	50-75	75-100	100-150	150-200	Total
Incremental Deposition (% of Applied)	1	14	5.7	2	0.9	0.6	1	0.2	0.2	0.1	25
	2	10	2.2	1	0.8	0.5	0.7	0.4	0.4	0.2	17
	3	20	5.5	3.2	2	0.9	0.9	0.3	0.3	0.1	33
	4	17	2.4	0.9	0.2	0.2	0.4	0.1	0.1	0.1	22
	5	13	1.8	0.8	0.3	0.3	0.2	0.1	0.2	0.1	17
	6	15	2.9	0.9	0.5	0.3	0.2	0.1	0.1	0.1	20
	7	7.3	4.5	3.3	2.3	2.4	0.8	0.7	0.5	0.5	22
	8	7.2	2.8	0.9	0.3	0.5	0.3	0.6	0.4	0.2	13
	9	8.1	3.6	1	0.4	0.5	0.4	0.6	0.4	0.4	15
	10	4.4	2.1	0.8	0.5	0.4	0.3	0.5	0.4	0.3	10
	11	5.8	2.1	0.9	0.5	0.8	0.4	0.6	0.4	0.4	12
	12	4.6	2.2	1	0.6	1.3	1.1	1.9	1.7	0.6	15

The downwind deposition was also expressed as the fraction of the material entering (Table 4), where the entering material is calculated as the total applied minus the amount deposited up to a

given distance. For example, the deposition from 20 to 30 m expressed as a fraction of the material entering is the integrated deposition from 20 to 30 m divided by that entering. The amount of material entering the 20 to 30 m distance is the total applied minus the in-swath deposition and the deposition from 0 to 20 m.

Table 4. Incremental deposition by distance and replication expressed as percentage of material entering each distance.

		Downwind Distance (m)								
	Rep	0-10	10-20	20-30	30-40	40-50	50-75	75-100	100-150	150-200
Incremental Deposition (% of Entering)	1	51	42	26	16	13	31	8.1	5.5	5.1
	2	47	20	11	9.7	7.1	12	7.5	7.5	4.4
	3	45	23	17	13	7.4	8	2.6	2.8	1.3
	4	50	15	6	1.4	1.4	3	0.7	0.8	0.8
	5	32	6.7	3.2	1.4	1.1	0.8	0.4	0.8	0.5
	6	30	8.7	3.1	1.6	1	0.6	0.2	0.3	0.2
	7	12	8.2	6.7	5.2	5.7	1.9	1.9	1.3	1.2
	8	19	9	3	1.2	1.9	1.2	2.5	1.3	0.9
	9	13	6.7	2	0.8	1.1	0.8	1.3	0.5	0.8
	10	7.9	4.1	1.7	1	0.9	0.7	1	0.8	0.7
	11	9.1	3.7	1.6	0.9	1.5	0.7	1.1	0.8	0.7
	12	8.6	2.2	1	0.6	1.3	1.1	1.9	1.7	1.4

3.3 Airborne Flux as Measured by Nylon Screens

The airborne dye mass flux presented in terms of percent of total applied is included in Table 5. The flux at all downwind distances was greater in the afternoon (replications 7-12) as compared to the morning (replications 1-6) partially as a result of increased wind speeds increasing transport distance of larger droplets.

Table 5. Total measured flux (through 0 to 6.1 m height) by distance and replication expressed as percentage of applied.

		Downwind Distance (m)								
	Rep	0-10	10-20	20-30	30-40	40-50	50-75	75-100	100-150	150-200
Total Measured Flux at Each Sampling Location (% of Applied)	1	5.4	3	2.7	5.3	9.3	3.3	2.4	1.9	0.3
	2	5	5.6	1.7	2.1	1.8	1.6	2.4	2.3	1.4
	3	17	7.9	6.5	3.8	4	1.2	0.8	0.3	0.3
	4	3.6	2.6	1	0.7	0.9	0.9	0.3	1.7	0.9
	5	6.1	3.9	3.1	2.6	2.6	19	1.4	0.9	0.8
	6	13.4	7	4.2	2.6	1.4	0.6	0.9	0.9	0.4
	7	29	23	10	11	7.6	7.6	6.3	7.3	4
	8	26	15	12	9.2	6.9	7.7	11	6.5	3.8
	9	20	21	15	13	6.7	6.3	7	5	3.3
	10	39	23	15	8.7	9	6.9	7.4	6.2	3.2

	11	24	15	7.9	7.9	5.8	3.4	5.5	5.9	4.5
	12	17	12	7.9	5.4	4.3	4.6	5.4	7.4	6.8

3.4 Water Sensitive Paper (WSP) Samples

Results from the WSP samples taken at 0, 3, and 6.1 m heights were averaged at each distance for each replication (Table 6). There was a rapid decrease in $D_{V0.5}$ with distance as the larger droplets settle out due to gravitational forces. The higher wind speeds in replications 7-12 caused larger droplets to be transported further downwind as compared to replications 1-6 with lower wind speeds. Although many of the cards measured no droplets at distances > 40 m, this should not be interpreted to mean that there were not droplets in the air. Droplet sizes less than 20 μm do not tend to result in a stained area that can be processed using image analysis. Additionally, the WSP data must be considered with the knowledge that the collection efficiency of the various droplet sizes varied with the wind speed. Based on work by May and Clifford (1967), the collection efficiency for a ribbon 2.54 cm wide for droplets of 200, 100, and 10 μm entrained in a 1 m/s airstream can be extrapolated as 76, 50, and .05% respectively, and likewise are 51, 19, and .004% respectively for droplets entrained in a 0.3 m/s airstream. The combination of very low collection efficiency for the smaller droplets, especially at the lower wind speeds (Reps 1-6) and the WSP lower droplet detection threshold contributed to the 0 $D_{V0.5}$ readings.

Table 6. Water sensitive paper measured droplet size at each sampling distance for each replication averaged over all three sampling heights (0, 3, and 6.1 m).

		Downwind Distance (m)								
	Rep	0-10	10-20	20-30	30-40	40-50	50-75	75-100	100-150	150-200
Droplet $D_{V0.5}$ by Replication (μm)	1	113	81	114	57	0	0	0	0	0
	2	77	82	67	66	58	43	11	0	0
	3	121	86	91	81	95	56	20	31	0
	4	76	59	30	12	0	0	11	12	0
	5	71	63	46	17	16	0	0	0	0
	6	107	75	55	37	0	0	12	0	0
	7	211	143	146	106	103	23	0	0	0
	8	98	76	66	79	32	11	14	0	0
	9	112	105	70	43	0	0	0	11	12
	10	111	90	72	39	22	0	0	0	0
	11	84	108	92	88	0	11	0	0	11
	12	91	93	48	15	0	0	0	12	0

3.5 Mass Accountability

Mass accountability was computed by comparing the mass of dye remaining in airborne (total mass of dye applied minus the total mass of dye deposited, both in-swath and downwind) to the dye mass flux past the 200 m sampling location as measured by the nylon screen samplers. The mass of dye not deposited on the mylar cards or sampled by the screen samplers was expressed as the percent of mass unaccounted for by the samplers used in this study (Table 7). The percent of mass unaccounted for increased dramatically from replication 1 (high RH and low wind speed) to replication 12 (low RH and high wind speed).

Table 7. Percent of total dye mass applied measured by each of the sampling methods and the percent of total dye mass applied of material unaccounted for passing the 200 m sampling location.

Replication	In-Swath (% Applied)	Deposition 0-200 (% Applied)	Airborne Flux at 200 m (% Applied)	Unaccounted (% Applied)
1	73	25	0.3	2.4
2	78	17	1.4	3.7
3	56	33	0.3	11
4	66	22	0.9	12
5	60	17	0.8	22
6	51	20	0.4	29
7	38	22	4.0	36
8	60	14	3.8	22
9	34	16	3.3	46
10	40	10	3.2	47
11	33	13	4.5	49
12	45	10	6.8	38

3.6 Correlation and Regression Analysis Results

Scatter plots of the initial correlation analysis results for the complete data set (replications 1-12) showed clustering in two discrete groups corresponding to the morning and the evening replications. The morning replications (1- 6) were conducted under cool, humid and calm conditions, while the evening replication (7 – 12) were conducted under hot, dry and windy conditions. This distinctive shift in the in-swath and the downwind deposition with respect to the time of day is readily apparent in the presented data (Table 2). Given that the meteorological parameters during each time period are highly correlated, the data was treated as two discrete cases, morning (replications 1-6) and evening (replication 7-12) for correlation and linear regression analysis.

In-swath deposition during the morning replications (1-6) was negatively correlated to wind speed at 2.5 m (PCC = -0.794, P = 0.05, n = 6; where PCC is Pearson's Correlation Coefficient) and positively correlated to relative humidity (PCC = 0.818, P = 0.04, n = 6). The best fit model for in-swath deposition includes relative humidity and wind speed (R^2 = 0.704). The fraction of

material unaccounted for was weakly correlated to the wind speed at 2.5 m (PCC = 0.773, P = 0.071, n = 6), highly and negatively correlated to relative humidity (PCC = -0.979, P = 0.0007, n = 6) and negatively correlated to the in-swath deposition (PCC = 0.834, P = 0.03, n = 6). The best fit model for unaccounted material included relative humidity and Ri (R^2 = 0.987). Though there were no significant correlations between downwind deposition and meteorological variables, the best fit model included relative humidity and wind speed (R^2 = 0.399). Other significant correlations for the morning data showed that downwind deposition in terms of fraction of material entering from 20 to 200 m was positively correlated to relative humidity (PCC's ranged from 0.858 – 0.916, with P's from 0.011 to 0.026, n = 6) and from 50 to 200 m was negatively correlated to wind speed at 2.5 m (PCC's ranging from -0.795 to -0.955, with P's from 0.003 to 0.05, n = 6).

The afternoon data set (replication 7 – 12) show no significant correlations other than a negative correlation between the unaccounted for material and the in-swath deposition (PCC = -0.921, P = 0.009, n = 6). The airborne flux at 200 m is weakly correlated to relative humidity, (PCC = 0.737, P = 0.09, n = 6) wind speed at 2.5 m, (PCC = -0.784, P = 0.06, n = 12) and Ri (PCC = 0.742, P = 0.09, n = 6). Regression analysis showed the best fit model for deposition included wind speed, relative humidity, and Ri (R^2 = 0.758), for in-swath deposition included relative humidity and Ri (R^2 = 0.900), and for the unaccounted material included wind speed, relative humidity, and Ri (R^2 = 0.762).

4. DISCUSSION AND CONCLUSIONS

Overall, the results generally showed greater in-swath and downwind deposition and less unaccounted for material and airborne flux at 200m for the morning replications versus the afternoon replications (Table 7). Lower wind speeds, cooler temperatures, and higher relative humidity during the morning replications likely resulted in less evaporation losses. The increased wind speeds, higher temperature, and lower humidity during the afternoon replications caused increased evaporation, smaller droplets and increased downwind movement. The flux measurements support these results with increased fluxes at all downwind distances in replications conducted during the afternoon (Table 4) as compared to the morning replications.

The amount of material unaccounted for was greater during the afternoon replications as a result of the lower relative humidity and higher wind speeds. A more detailed examination of the screen measured data suggested that the sampling height was not sufficient to capture the entire plume, which would have resulted in a greater amount of material unaccounted. The screen concentrations at 100, 150, and 200 m shows an increasing flux gradient with height with slopes ranging from 0 to 0.007 $\mu g/cm^2$ per m. These slopes were generally an order of magnitude higher during the afternoon replications. Statistical analysis over replications indicated a positive correlation between the material unaccounted and the screen flux slopes (PCC = 0.661, P = 0.0375, n = 12).

No single meteorological factor dominated the deposition or flux of the aerial spray treatments replicated in this study, rather, an interaction of the all of the meteorological parameters

influence the ultimate fate the aerially applied sprays. Generally, decreases in relative humidity decreased downwind deposition and increased the amount of unaccounted for spray material due to evaporative effects decreasing droplet size. Increasing wind speeds decreased in-swath deposition and when coupled with low relative humidity and increased stability, decreased total downwind deposition. Increases in stability were only moderately correlated to downwind deposition and to flux measurements past 40 m. Though this data set covers a limited range of meteorological conditions, the trends demonstrated hold from the standpoint of the system physics and previous literature and provide applicators with a further understanding of the relationships between spray transport and deposition and local meteorology.

These results have implications for both researchers and aerial applicators. The authors have tried to account for collection efficiency effects and recovery rates for the sampling media used in this study. This fundamental understanding of the collectors used in a study is needed for every type of sampler and particularly, when using less well documented or novel collectors in their work. Aerial applicators are aware that varying meteorological conditions greatly affect the amount of in-swath deposition and spray drift. Many of the new agrochemicals have greatly reduced rates of active ingredients as compared to older materials. Therefore, the dramatic differences found in these studies may result in a product being effective in the morning but not in the afternoon if no changes in application parameters, such as droplet size or spray formulation, are made.

5. ACKNOWLEDGEMENTS

Thanks to the Aerial Application Technology team members, S. Harp, C. B. Harris, P. C. Jank, J. D. Lopez, C. Parker, and L. Denham who provided essential support for the field studies.

6. REFERENCES

ASAE Standards. 2000. S572 AUG99: Spray nozzle classification by droplet spectra. St. Joseph, Mich.: ASAE.

Bache, D. H., and D. R. Johnstone. 1992. Microclimate and Spray Dispersion. New York, N.Y.: Ellis Horwood.

Bird, S. L. 1995. A compilation of aerial spray drift field study data for low-flight agricultural application of pesticides. In Environmental Fate Studies: State of the Art, 195-207. M. L. Leng, E. M. K Loevey, and P. L. Zubkoff. eds. Chelsea, Mich.: Lewis Publishers.

Bird, S. L., D. M. Esterly, and S. G. Perry. 1996. Atmospheric pollutants and trace gases. J. Environ. Quality 25(5): 1095-1104.

Craig, I., N. Woods, G. Dorr. 1998. A simple guide to predicting aircraft spray drift. Crop Protection 17(6):475-482.

Fritz, B. K. and W. C. Hoffmann. 2008. Collection efficiencies of various airborne spray flux samplers used in aerial application research. J. ASTM Int. 5(1)

Frost, K. R. 1973. Pesticide drift from aerial and ground applications. Agric. Eng., 51(8): 460-464.

Hoffmann, W. C., B. K. Fritz and D. E. Martin. 2007. AGDISP sensitivity to crop canopy characterization. Trans. ASABE. Accepted for publication.

Karsky, T. J. and G. Thomasson. 1989. Study of downwind drift from agricultural aircraft. ASAE Paper No. AA89-003. Presented at the NAAA/ASAE Joint Technical Session in New Orleans, Louisiana, December 6, 1989. St. Joseph, MI.

May, K. R., and R. Clifford. 1967. The impaction of aerosol particles on cylinders, spheres, ribbons, and discs. *Annuals of Occupation Hygiene* 10(1): 83-95.

Payne, N. J. and D. G. Thompson. 1992. Off-target glyphosate deposits from aerial silvicultural applications under various meteorological conditions. Pestidicide Science. 34:53-59.

Salyani, M., Farooq, M., and Sweeb, R. D. 2007. Mass balance of citrus spray applications. ASABE Paper No. 071037. St. Joseph, MI.5

SAS. 2001. Release 8.02. Cary, N.C.: SAS Institute, Inc.

Thistle, H. W., Teske, M. E., Droppo, J. G., Allwine, C. J., Bird, S. L., Londergan, R. J. 2005. AGDISP as a source term in far field atmospheric transport modeling and near field geometric assumptions. ASAE Paper Number 051149. St. Joseph, MI.

Van den Berg, F., R. Kubiak, W. G. Benjey. 1999. Emission of pesticides into the air. Water, Air, and Soil Pollution 115, 195-218.

Ware, G. W., W. P. Cahill, P. D. Gerhardt, and J. M. Witt. 1970. Pesticide drift IV. On target deposition from aerial applications of insecticides. J. Econ. Entomology, 63(6): 1982-1983.

Willis, G. H., and L. L. McDowell. 1987. Pesticide persistence on foliage. Rev. Environ. Contamin. Toxicol. 100:22.